



# Preconditioning of the immune system modulates the response of papillary thyroid cancer to immune checkpoint inhibitors

Fabiana Pani <sup>1,2</sup> Yoshinori Yasuda <sup>3,4</sup> Sylvie T Rousseau <sup>1</sup>,  
Kevin C Bermea,<sup>1</sup> Solmaz Roshanmehr,<sup>4</sup> Rulin Wang,<sup>5</sup>  
Srinivasan Yegnasubramanian,<sup>5</sup> Patrizio Caturegli,<sup>4</sup> Luigi Adamo <sup>1</sup>

**To cite:** Pani F, Yasuda Y, Rousseau ST, *et al.* Preconditioning of the immune system modulates the response of papillary thyroid cancer to immune checkpoint inhibitors. *Journal for ImmunoTherapy of Cancer* 2022;**10**:e005538. doi:10.1136/jitc-2022-005538

► Additional supplemental material is published online only. To view, please visit the journal online (<http://dx.doi.org/10.1136/jitc-2022-005538>).

FP and YY contributed equally.  
Accepted 15 November 2022



© Author(s) (or their employer(s)) 2022. Re-use permitted under CC BY-NC. No commercial re-use. See rights and permissions. Published by BMJ.

For numbered affiliations see end of article.

**Correspondence to**  
Dr Luigi Adamo;  
ladamo2@jhmi.edu

## ABSTRACT

**Background** The response of solid tumors such as papillary thyroid cancer (PTC) to immune checkpoint inhibitors (ICIs) is highly variable. The biological basis of this variability remains unknown.

**Methods** To test the hypothesis that preconditioning of the immune system modulates the therapeutic effect of ICIs, we used a murine model where PTC and iodine exacerbated thyroiditis (IET) can be induced in a temporally predictable fashion. A total of 122 mice were divided into 3 experimental groups. In the first one, named concomitant IET and PTC (No.=40), IET, and PTC were induced at the same time; in the second one, named pre-existing IET (No.=44), IET was induced prior to the induction of PTC; in the third one, named no IET (No.=38), only PTC was induced. Following disease induction, mice of each group were treated with anti-PD-1 antibody, anti-lymphocyte activation gene 3 antibody (anti-Lag3), anti-T-cell immunoglobulin and mucin domain 3 antibody (anti-Tim3), or IgG control. Ten weeks after the initial ICI injection, mice were sacrificed to collect the thyroid gland for histological analysis, to quantify the incidence and burden of PTC, and to perform high-throughput single-cell RNA sequencing of infiltrating CD45<sup>+</sup> cells.

**Results** In the concomitant IET and PTC group, ICI treatment reduced PTC incidence ( $p=0.002$  comparing treatment with any ICI vs control), while it had no effect in the pre-existing IET and no IET groups. Single-cell sequencing of thyroidal CD45<sup>+</sup> cells showed that the different ICIs tested had both specific and shared effects on all the components of the thyroidal immune cell infiltrate. The shared effect of the tested ICIs was dependent on the presence of pre-existing versus concomitant IET. In the context of concomitant IET, ICI treatment resulted in the modulation of a greater number of pathways related to both innate and adaptive immunity.

**Conclusions** Response to ICIs depends on the status of the immune system of the treated individual. Modulation of the immune system should be explored as a tool to improve response to ICIs in patients with PTC or other forms of cancer.

## WHAT IS ALREADY KNOWN ON THIS TOPIC

⇒ The tumor-controlling effect of immune checkpoint inhibitors (ICIs) is highly variable across patients. The etiological basis of this variability is unknown. Body composition, prior antibiotic treatment, gut microbiota composition, genetic susceptibility to autoimmunity, tumor irradiation, and development of thyroiditis after exposure to ICIs have all been associated with changes in the clinical response to ICI treatment.

## WHAT THIS STUDY ADDS

⇒ Using a murine model that allows us to induce in a temporally predictable fashion papillary thyroid cancer (PTC) and iodine exacerbated thyroiditis (IET), we found that the presence of recent IET, as opposed to pre-existing IET, was associated with a stronger effect of ICIs on both adaptive and innate immunity, and a stronger ‘tumor controlling’ effect. These findings suggest that the immune status of the treated individual at the time of administration of ICIs modulates the response to ICIs.

## HOW THIS STUDY MIGHT AFFECT RESEARCH, PRACTICE OR POLICY

⇒ Our findings suggest that modulation of the inflammatory milieu and thus the immune system might be used as a tool to increase the clinical response to ICIs. Since we used a murine model of PTC and IET, our findings point to the need to perform human studies to understand whether induction of thyroiditis with the administration of iodine might be a useful adjuvant treatment to improve response to ICIs in patients with PTC. However, the biological paradigm we propose is likely relevant also to other types of cancer. Therefore, our work calls for additional pre-clinical and clinical studies aimed at understanding whether activation of the immune system, via induction of thyroiditis or other means, could be a useful strategy to improve response to ICIs in oncological patients.

## BACKGROUND

Immune checkpoint inhibitors (ICIs) have revolutionized the treatment of oncologic

patients.<sup>12</sup> However, patients' response to ICI treatment is highly variable. Some patients experience dramatic clinical responses while others have minimal or no response. The etiological basis of this marked variability in clinical response across individuals remains mostly unknown. Body composition,<sup>3</sup> prior antibiotic treatment,<sup>4</sup> gut microbiota composition,<sup>5</sup> genetic susceptibility to autoimmunity,<sup>6</sup> tumor irradiation,<sup>7</sup> and development of thyroiditis after exposure to ICIs<sup>8–10</sup> have all been associated with changes in the clinical response to ICI treatment, but a comprehensive hypothesis to explain these observations is lacking.

All the factors referenced above modulate the host immune system at the peritumoral and/or systemic level. Therefore, in our opinion, these observations raise the intriguing possibility that modulation or pre-conditioning of the immune milieu might be an important determinant of response to ICI.

We recently described a murine model that allows us to induce, in a temporally predictable fashion, papillary thyroid cancer (PTC) and thyroiditis. This model, called NOD.H2<sup>h4</sup> TPO-CRE-ER BRAF<sup>v600E</sup>, develops PTC on exposure to tamoxifen and develops iodine exacerbated thyroiditis (IET) on iodine administration.<sup>11</sup> Here, we take advantage of this model to test the hypothesis that immune preconditioning via induction of IET can modulate response to ICIs. Since we were interested in investigating a 'class effect' more than the response to a specific therapeutic agent, we did a parallel study of the response to three different ICIs, blocking antibodies targeting programmed death-1 (PD-1),<sup>12</sup> blocking antibodies targeting lymphocyte activation gene 3 (LAG-3)<sup>13</sup> and blocking antibodies targeting T-cell immunoglobulin and mucin domain 3 (TIM-3).<sup>14</sup>

To increase the sensitivity of our analysis, we compared responses to ICIs in three different conditions: animals with PTC but without IET; animals who developed IET before developing PTC ('pre-existing IET'); and animals who developed PTC at the same time in which they developed IET ('concomitant IET'). Our findings indicate that the response to ICI is markedly modulated by host immune preconditioning.

## METHODS

### Experimental study groups

A total of 122 double-mutant NOD.H2<sup>h4</sup> TPO-CRE-ER BRAF<sup>v600E</sup> were developed by breeding and injected with tamoxifen to induce PTC, as previously described.<sup>11</sup> Mice were separated into three groups according to the administration of sodium iodide in the drinking water and its timing. In the first group labeled as 'concomitant IET' (No.=40), sodium iodide administration was begun at 8 weeks of age concurrently with the tamoxifen injections and continued for 12 weeks. In the second group, 'pre-existing IET' (No.=44), sodium iodide was given first from weeks 8 to 20 of age, and then tamoxifen injections were started at 20 weeks of age. In the third group, 'no

IET' (No.=38), no sodium iodide was administered, and tamoxifen injections began at 8 weeks of age.

In each group, mice were treated with one of three ICIs or with isotype control. In particular, 19 animals received anti-TIM-3 antibodies, 6 in the concomitant IET arm, 7 in the pre-existing IET arm, and 6 in no IET arm. 22 animals were treated with anti-PD-1 antibodies, 8 in the concomitant IET arm, 7 in the pre-existing IET arm, and 7 in the no IET arm. Twenty-three animals were treated with anti-LAG-3 antibodies, 8 in the concomitant IET arm, 9 in the pre-existing IET arm, and 6 in the no IET. Fifty-eight animals were included in the control group, 18 in the concomitant IET arm, 21 in the pre-existing IET arm, and 19 in the no IET arm. Most of the animals in the control group received injections of isotype control antibodies. A subgroup of control animals did not receive isotype control antibodies and overlapped with the control cohort published in our previous report.<sup>11</sup> The experimental design of all 122 mice is summarized in [figure 1](#). All mice were sacrificed 10 weeks after the first antibody injection.

### Treatment with ICIs

ICI antibodies were administered via intraperitoneal injection between 24 and 36 weeks of age. All animals received ICIs about 4 weeks after completion of tamoxifen treatment and about 10 weeks prior to sacrifice. Antibodies (online supplemental table 1) were diluted in a specific dilution buffer (InVivo Pure<sup>TM</sup> BioXCell pH. 7.0 IP0070) to a final concentration of 250 µg/200 µL and stored at 4°C. Each mouse was injected intraperitoneally with 200 µL of this solution three times, once every 2 days.

### Thyroid histopathology

At sacrifice, thyroid glands were resected and prepared for histopathology (hematoxylin and eosin [H&E] stain) and/or flow cytometry. For H&E histopathology, the thyroid glands or lobes were fixed for 24 hours in Beckstead solution<sup>15</sup> and embedded in paraffin. In 74 mice, the entire gland was used for this purpose. In the remaining 48, the right lobe was used for histopathology and the left lobe for flow cytometry and single-cell proteogenomic analysis. Thyroid blocks were cut into 5 µm sections, stained with H&E, and imaged using a digital microscope (Olympus BX43) equipped with the Cell Sens Standard software. The images were then scored for PTC and thyroiditis by an experienced pathologist blinded to experimental group assignments. For immunohistochemistry, thyroid sections were deparaffinized and rehydrated as described,<sup>11</sup> then stained using rabbit anti-mouse B220 antibody clone RA3.

### Flow-cytometry and singlecell proteogenomic analysis

Animals with pre-existing or concomitant IET were analyzed on different days. On each day, one lobe of the thyroid gland of two mice per each experimental condition (isotype treatment vs PD-1 treatment vs LAG-3 treatment vs TIM-3 treatment) was digested to prepare

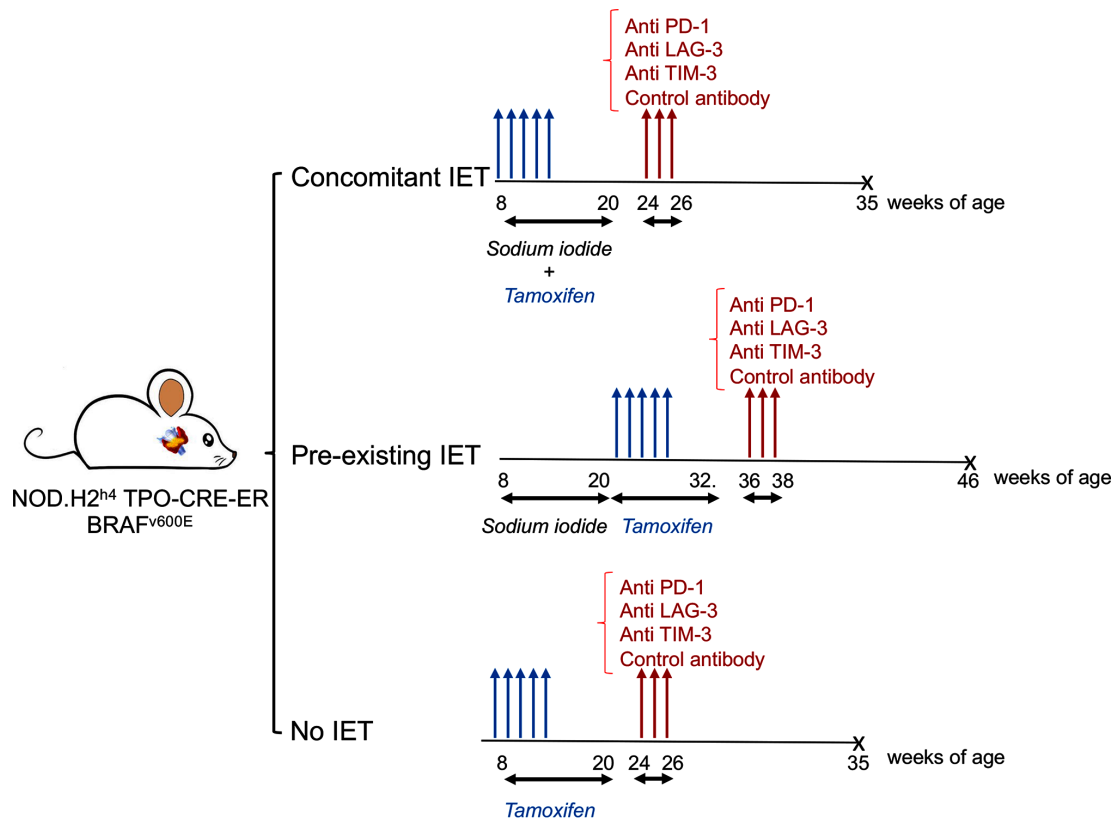


**Figure 1** Experimental design. NOD.H2<sup>h4</sup> TPO-CRE-ER BRAF<sup>v600E</sup> mice were divided into three experimental arms. In the first arm, tamoxifen was administered starting at 8 weeks of age to induce papillary thyroid cancer (PTC). At the same time, water was supplemented with sodium iodide to trigger iodine exacerbated thyroiditis (IET). In the second arm, sodium iodide was administered starting at 8 weeks of age, but tamoxifen was administered starting at 20 weeks of age, after completion of 12 weeks of sodium iodide treatment. In the third arm, tamoxifen treatment was started at 8 weeks of age and no sodium iodide was administered. About 2 weeks after completion of treatment with tamoxifen, ICIs were administered. X: All mice were sacrificed approximately 10 weeks after the initial antibody injection. ICI, immune checkpoint inhibitor.

a single-cell suspension, as previously described.<sup>11</sup> The tissue was minced and digested for 2 hours at 4°C and then for 30 min at 37°C in a solution of RPMI 1640. During digestion, 2 drops of Vibrant Dye Cycle Violet Ready Flow Reagent (DCV-Invitrogen) were added to each half thyroid to stain metabolically active cells. At the end of the digestion, cells were washed, filtered through a 40 µm strainer, resuspended in approximately 250 µL of FACS buffer, and treated with Fc block (BioLegend, 1:100) for 15 min on ice, and then stained with CITE-Seq antibodies (Mission Bio). To this end, first, each sample was stained with BioLegend 160X Universal Immune Cell Mix. One pouch of lyophilized reagents was resuspended in 50 µL of a dedicated buffer according to the manufacturer's instructions and 12 µL of antibody suspension was used to stain cells from each condition. Directly after adding the 160X-plex antibody mix, cells from each treatment condition were stained with 5 µL of a 1:10 dilution of BioLegend Hashtag-C antibodies. For the four different experimental conditions, Hashtags 1, 2, 4, and 5 were used, respectively. At this point, a PE-labeled antibody against CD45 (BioLegend, clone 30-F11) was added to each sample at 1:200 dilution. After 30 min of incubation on ice, samples were washed and strained. Immediately

prior to sorting Propidium Iodide was added to each sample and CD45<sup>+</sup>, DCV<sup>+</sup>, and PI cells were sorted in DMEM with 1% FCS using a MoFlo cell sorter. After sorting, cells from the four experimental conditions were pooled together in a 1 : 1 : 1 : 1 ratio. They were spun down, counted using trypan blue, and partitioned into droplets using the 10X Genomics Chromium Controller using 40,000 cells (superloading) per pooled sample. Single cell libraries for 5' Digital Gene Expression, and feature barcodes including sample hashtags, were produced using 10X Genomics Chromium Next GEM Single Cell 5' Library and Gel Bead Kit v1.1 according to manufacturer instructions. The feature barcode library was sequenced at a depth of 15,000 reads per cell. The gene expression library was sequenced at a depth of 50,000 reads per cell. Next-generation sequencing was performed through the Johns Hopkins Sidney Kimmel Comprehensive Cancer Center's Experimental and Computational Genomics Core using the NovaSeq 6000 platform.

#### Statistical analysis of histology data

Data were analyzed using GraphPad Prism V.9.3.1. The presence or absence of PTC across experimental groups was compared using the  $\chi^2$  test.

## Analysis of singlecell sequencing data

Analysis of singlecell sequencing was performed in Partek Flow software (V.10.0). Raw sequencing reads were first processed using the Cell Ranger package from 10X Genomics, excluding introns, and reads were aligned to the mm10 reference mouse genome. Filtering was carried out to remove cells with low read counts and doublets, and demultiplexing was accomplished using hashtag oligos, resulting in a count of 30,001 cells between 2 samples. Next, the pooled data from the 2 samples were normalized for read depth by counts per million and CITE-seq weighted-nearest-neighbor was used to integrate the gene expression and protein datasets. Then, principal component analysis was performed, and the scree plot was used to estimate the minimum number of PCs with which to move forward. Dimensionality reduction and visualization was carried out using uniform manifold approximation and projection (UMAP). We used graph-based clustering (Louvain clustering algorithm; Resolution of 0.5; Euclidean distance metric) considering only gene expression data to identify cell clusters with significant differences in gene expression profiles.

At this stage, we applied biological knowledge to identify the cell types present in each visual cluster. We first compared the genes highly expressed in each cluster with the immune cell gene expression data in the IMMGEN database ([www.immgen.org](http://www.immgen.org)). We integrated this analysis with the expression of surface markers as detected by CTIE-Seq antibodies. More specifically, we used: positive staining with CD19 antibody to confirm the identity of the B cell cluster; positive staining with CD3, CD4, or CD8 antibody to confirm the identity of the T cell cluster; positive staining with Ly6G and CD11b antibodies to confirm the identity of the neutrophil cluster; positive staining with CD11b, CD11c, and F4-80 antibodies to confirm the identity of macrophages; and positive staining with CD11c and negative staining with F4-80 antibodies to confirm the identity of dendritic cells. Annotation of cell types was 'published' to the whole analysis pipeline. Analysis of variance was used to compare gene expression across specific cell clusters or experimental conditions. KEGG pathway analysis of differentially expressed genes was performed using DAVID bioinformatics resources.<sup>16</sup>

## RESULTS

### In the presence of concomitant iodine-induced thyroiditis, PTC responds better to ICIs

The incidence of PTC at the time of thyroid harvesting/terminal sacrifice in mice receiving the isotype control was similar to what we observed in our initial report<sup>11</sup> (figure 2), being highest in the concomitant IET group (18 of 18, 100%), intermediate in the no IET group (16 of 19, 84%), and reduced in the pre-existing thyroiditis group (11 of 21, 52%, figure 2, gray bars). Administration of any of the three ICIs significantly reduced PTC incidence as compared with the isotype control in the concomitant IET group, where only 4 of 6 (67%) TIM-3

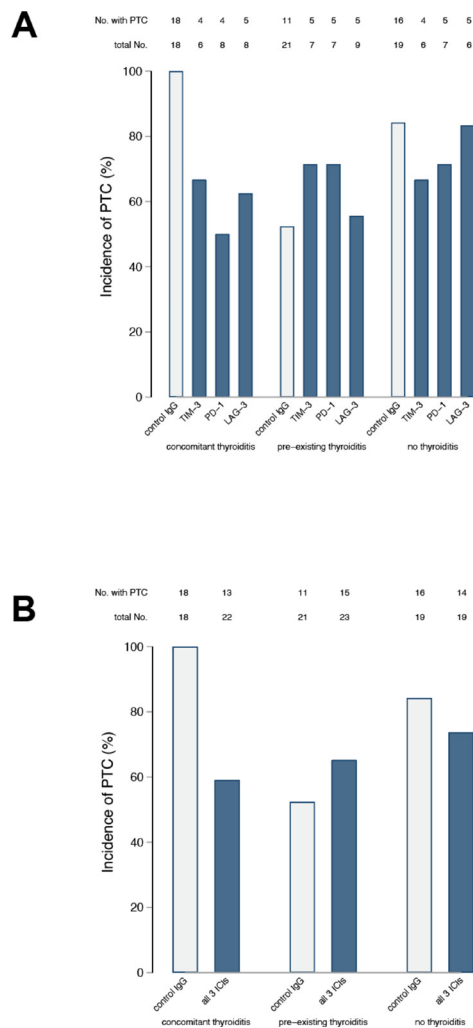


**Figure 2 Therapeutic response to ICI is dependent on immune preconditioning.** After sacrifice, thyroids were isolated from all animals and histological sections were stained with H&E. The presence or absence of PTC was assessed by a pathologist blinded to study group assignment. The number of animals with PTC present or absent is reported for each study arm .A) Within each study arm, results are broken down by treatment group (anti-TIM-3 Ab, anti-PD-1 Ab, anti-LAG-3 Ab, or control). Analysis via the chi-square test showed that the frequency of PTC was different across experimental groups in the context of concomitant IET ( $p=0.018$ ) but not in the context of no IET ( $p=0.761$ ) or pre-existing IET ( $p=0.725$ ). B) All animals treated with ICI are combined within the same group. Also in this analysis the frequency of PTC was lower in presence of concomitant IET ( $p=0.002$ ) but not in the presence of pre-existing IET ( $p=0.387$ ) or in the absence of IET ( $p=0.426$ ). ICI, immune checkpoint inhibitor; IET, iodine exacerbated thyroiditis; LAG-3, lymphocyte activation gene 3; PTC, papillary thyroid cancer; TIM-3, T-cell immunoglobulin and mucin domain 3.

blocked mice, 4 of 8 (50%) PD-1 blocked mice, and 5 of 8 (63%) LAG-3 blocked mice were found to have PTC at sacrifice (figure 2A,  $p=0.017$  by  $\chi^2$  test). ICI administration, instead, had no beneficial effect in mice of the pre-existing thyroiditis or no thyroiditis groups ( $p=0.725$  and  $0.761$ , respectively, figure 2A). Combining the three types

of ICIs into one at the time of analysis yielded similar results: as compared with the isotype control, at the time of organ harvesting PTC was less common in the concomitant IET group treated with ICIs ( $p=0.002$ , [figure 2B](#)), whereas its incidence was similar to the isotype control in the pre-existing IET ( $p=0.387$ ) or no IET ( $p=0.426$ ) groups treated with ICIs ([figure 2B](#)).

The severity of PTC, as judged by the number of neoplastic foci present in the thyroid gland, mimicked the incidence results reported above. In mice receiving the isotype control, two or more foci of PTC were highest in concomitant IET (13 of 18, 72%), lower in no IET (12 of 19, 63%), and lowest in pre-existing IET (2 of 21, 9%, [table 1](#)). Administration of any of the three ICIs reduced PTC severity in mice with concomitant IET ( $p=0.107$ , [table 1](#)), but had no effect in the no IET ( $p=0.974$ ) or pre-existing IET ( $p=0.242$ ) groups. The stronger clinical effect of ICI in the context of concomitant IET was clearer when animals treated with any ICI were pooled within the same group. Comparing control-treated animals to animals treated with any ICI, treatment was associated with a clear reduction in the frequency of multifocal PTC in the context of concomitant IET ( $p=0.008$ ) but not in the context of no IET ( $p=0.71$ ) or pre-existing IET ( $p=0.07$ ).

#### Presence of pre-existing versus concomitant IET is associated with marked changes in the composition of the PTC-associated immune cell infiltrate in the thyroid, treatment with ICIs is not

To gain insight into this finding, we decided to use single-cell proteogenomic analysis to investigate the thyroid immune infiltrate in our different experimental groups. We focused on animals with pre-existing or concomitant IET to avoid bias induced by induction of thyroiditis.

[Figure 3](#) shows three-dimensional UMAP plots of the immune infiltrate in animals with concomitant or pre-existing IET treated with isotype control antibody or each of the three tested ICIs. The presence of concomitant versus pre-existing IET resulted in a marked variation in the composition of the thyroidal immune infiltrate. As compared with concomitant IET, pre-existing thyroiditis was in fact associated with a clear expansion of B cells and T cells, and with a marked shift in the gene expression profile of Ly6G<sup>+</sup> neutrophils ([figure 3A and 3E](#)). In the context of concomitant IET, treatment with any of the tested ICIs did not result in obvious changes in the relative representation of the identified cell types ([figure 3A and 3B and 3C and 3D](#)). This was also true in the context of pre-existing IET ([figure 3E and 3F and 3G and 3F](#)). To corroborate this observation with performed immunohistochemistry (IHC) for the B cell marker B220. Online supplemental figure S2 shows that IHC confirmed that pre-existing IET was characterized by a significant prevalence of B cells while concomitant IET had very scarce B cells, and this finding was consistent across treatment groups.

**Table 1** Focality of papillary thyroid cancer in NOD. H2<sup>h4</sup> TPO-CRE-ER BRAF<sup>v600E</sup> mice treated with immune checkpoint inhibitors (ICIs), according to the status of iodine-exacerbated thyroiditis (IET)

	No of mice	Papillary thyroid cancer foci			P value
		None	One	≥2	
Concomitant IET: 0.107					
Control	18	0	5	13	
LAG-3 Ab	8	3	2	3	
PD-1 Ab	8	4	1	3	
TIM-3 Ab	6	2	1	3	
No IET: 0.974					
Control	19	3	4	12	
LAG-3 Ab	6	1	1	4	
PD-1 Ab	7	2	1	4	
TIM-3 Ab	6	2	1	3	
Pre-existing IET: 0.242					
Control	21	10	9	2	
LAG-3 Ab	9	4	3	2	
PD-1 Ab	7	2	1	4	
TIM-3 Ab	7	2	2	3	
	No of mice	Papillary thyroid cancer Foci			P value
		None	One	≥2	
Concomitant IET: 0.008					
Control	18	0	5	13	
ICI	22	9	4	9	
No IET: 0.70					
Control	19	3	4	12	
ICI	19	5	3	11	
Pre-existing IET: 0.07					
Control	21	10	9	2	
ICI	23	8	6	9	

The data are reported both separating by specific ICIs (top) and condensing all ICI-treated animals within the same group (bottom). The P column reports the p value for the  $\chi^2$  test. LAG-3, lymphocyte activation gene 3; PD-1, programmed death-1; TIM-3, T-cell immunoglobulin and mucin domain 3.

#### Gene expression alterations induced by treatment with different ICIs have both common and specific features

In our experimental design, within each experimental condition (pre-existing vs concomitant IET) we have three different ICI treatments. This allowed us to compare the response to different ICIs and, through this, identify molecular signatures that are common to all tested ICIs and therefore are likely critical for the observed therapeutic effect.

With this in mind, we first compared the gene expression changes induced by treatment with anti-PD-1 antibody

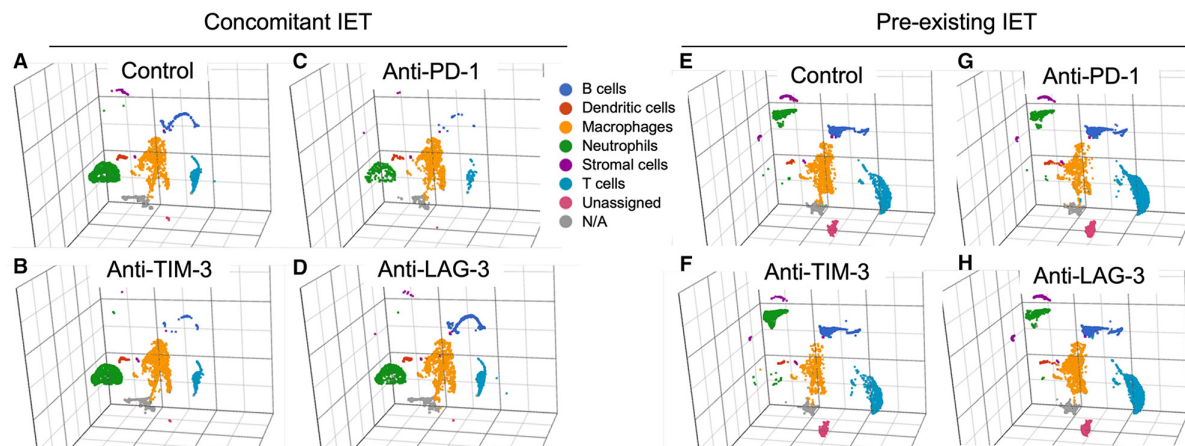


**Figure 3** Immune preconditioning modulates the composition of the thyroidal immune cell infiltrate, treatment with ICIs does not. UMAP plot representing the gene expression profile of CD45<sup>+</sup> cells isolated from the thyroids of animals with concomitant IET (A–D) or pre-existing IET (E–H). The thyroids from two animals for each experimental condition were digested and CD45<sup>+</sup> cells were sorted by flow cytometry. Cells from each experimental condition were labeled with hashtag antibodies and pooled into a single reaction/sequencing library per experimental arm. Immune cell types were identified by unsupervised graph-based clustering integrated with biological knowledge. Six different immune cell types were identified: B cells, dendritic cells, macrophages, neutrophils, stromal cells, and T cells. A small fraction of CD45<sup>+</sup> cells did not fall into any of these six categories and was labeled as unassigned or N/A. The relative representation and the global gene expression profile of the 6 different immune cell types identified appeared to be markedly different in “Control concomitant IET” and “Control pre-existing IET” (A vs E). However, within each experimental arm, treatment with the different tested ICIs did not appear to induce marked changes in the relative representation or in the global gene expression profile of any of the identified immune cell types (i.e., plot A is similar to plots B–D while plot E is similar to plots F–H). ICI, iodine exacerbated thyroiditis; IET, iodine exacerbated thyroiditis; N/A, not available; UMAP, uniform manifold approximation and projection. PD-1, programmed death-1; LAG-3, lymphocyte activation gene 3; TIM-3, T-cell immunoglobulin and mucin domain 3.

to the gene expression changes induced by other treatments using hierarchical clustering/heatmap analysis. Figure 4A,C depict heatmap representations of the genes differentially expressed in PD-1-treated animals versus control animals (FDR<0.05, fold change >1.5 or <1.5). The heatmaps show that the effect of treatment with anti-PD-1 antibody was for the most part specific to PD-1. In fact, only a fraction of the genes modulated by PD1 were modulated similarly by the two other ICIs tested. This was true both in the context of concomitant IET (figure 4A) and in the context of pre-existing IET (figure 4C). As a sensitivity analysis, we looked at differential gene expression across the four treatment groups within specific cell populations. Online supplemental figure S1 shows that both in animals with pre-existing IET and in animals with concomitant IET, treatment with different ICIs resulted in treatment-specific gene expression changes in B cells, neutrophils, macrophages, and T cells.

To gain insight into this observation we performed a Venn diagram-based analysis of all the genes differentially expressed between isotype control-treated, anti-TIM-3 treated, anti-PD-1 treated, and anti-LAG-3 treated animals in the two experimental conditions (FDR<0.05). Figure 4B shows that anti-TIM-3 treatment was associated with a change in the expression of 3265 genes as compared with isotype control-treated animals. Treatment with anti-LAG-3 antibody was associated with a change in the expression of 3658 genes as compared with isotype control-treated animals. Treatment with anti-PD-1 antibody was associated with a change in the expression

of 9962 genes as compared with isotype control-treated animals. Notably, as compared with isotype control-treated animals only 1193 genes were affected by all the three different ICIs studied. Figure 4D reports a similar analysis performed within the thyroidal immune infiltrate of animals with pre-existing IET. In this case, anti-TIM-3 treatment was associated with a significant change in the expression of 9167 genes as compared with isotype control-treated animals. Treatment with anti-LAG-3 antibody was associated with a change in the expression of 3738 genes as compared with isotype control-treated animals. Treatment with anti-PD-1 antibody was associated with a change in the expression of 6384 genes as compared with isotype control-treated animals. Only 2835 genes were affected by all the three different ICIs studied.

#### The ‘shared’ set of genes modulated by all ICIs changes in response to immune preconditioning

All tested ICIs had a ‘therapeutic’ effect in mice with concomitant IET but not in mice with pre-existing IET. To gain insight into the interaction between immune preconditioning and ICI treatment, we performed a Venn diagram-based comparison of the genes modulated by all tested ICIs in animals with pre-existing IET and in animals with concomitant IET. Figure 5 shows that there was little overlap between the two groups of genes. 59.6% (711 of 1193) of genes modulated by all ICIs in the context of concomitant IET were not modulated by ICIs in the context of pre-existing IET. 83% (2353 of 2835) of genes modulated by all ICIs in the context of

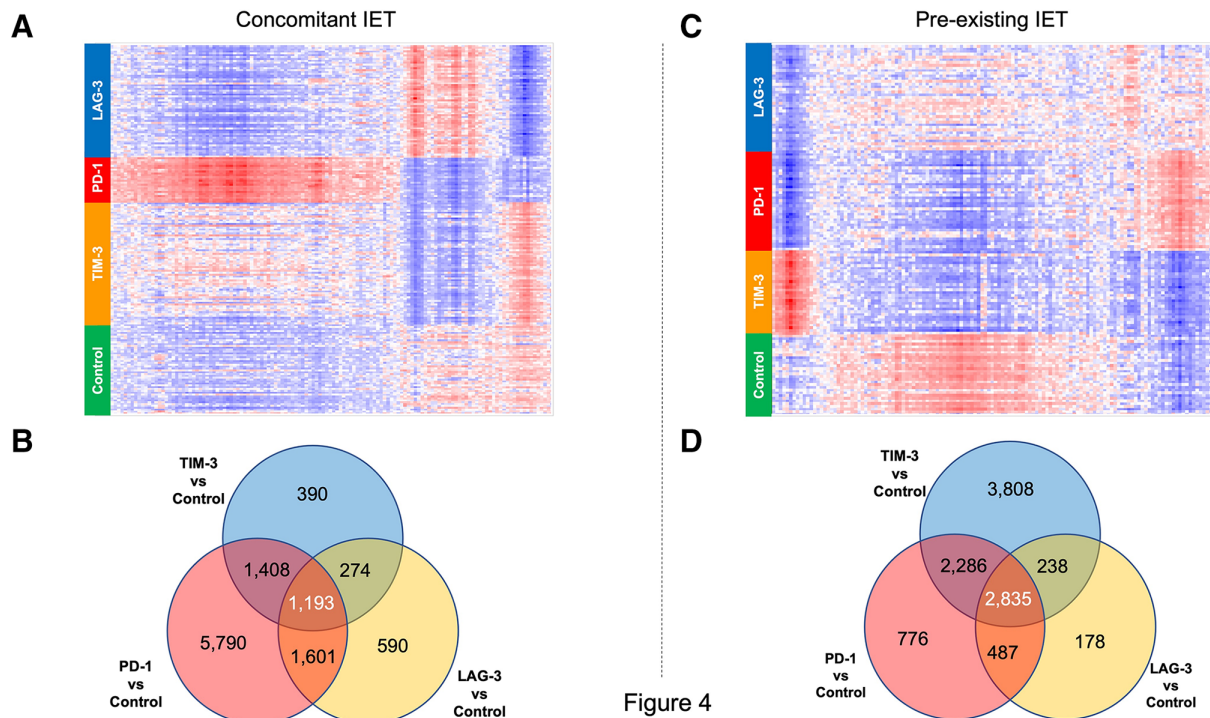


Figure 4

**Figure 4** Different immune checkpoint inhibitors (ICIs) have both distinct and shared effects on the gene expression profile of thyroidal CD45<sup>+</sup> cells. Differential gene expression analysis from CD45<sup>+</sup> cells isolated from the thyroid of experimental animals. (A, B) Data collected from the analysis of animals in the concomitant IET experimental arm. (C, D) Data collected from the analysis of animals in the pre-existing IET experimental arm. (A, C) Hierarchical clustering/heatmap of genes differentially expressed with FDR < 0.05 and fold change > 1.5 between animals treated with anti-PD-1 and controls. The heatmaps show that the effect of the 3 different ICIs on this set of genes is different for each ICI, both in the concomitant IET experimental arm and in the pre-existing IET experimental arm. Red indicates upregulation and blue indicates downregulation. (B, D) Venn diagram analysis of genes differentially expressed with FDR < 0.05 between anti-TIM-3 (TIM-3) treated cells and isotype control (Iso), anti-PD-1 (PD-1) treated cells and isotype control, and anti-LAG-3 treated cells (LAG-3) and isotype control. The Venn diagram shows that only a fraction of the genes modulated by each ICI is modulated by all ICIs. This observation was consistent across the two experimental arms. IET, iodine exacerbated thyroiditis; PD-1, programmed death-1; LAG-3, lymphocyte activation gene 3; TIM-3, T-cell immunoglobulin and mucin domain 3.

pre-existing IET were not modulated in the context of concomitant IET. Only 482 genes were modulated by all ICIs both in the context of pre-existing and concomitant IET. Pathway enrichment analysis showed that in the context of concomitant IET, ICIs modulated several critical pathways related to the immune system that were not modulated in the context of pre-existing IET (figure 5B and 5A and 5C).

## DISCUSSION

We used a murine model that allows induction of PTC and IET in a temporally controlled fashion to investigate the effect of immune preconditioning on the response to ICIs (figure 1). We found that immune preconditioning modulates the tumor-controlling effect of ICIs (figure 2, table 1). This is likely the most important and clinically relevant finding of our study. Expanding on this observation, we found evidence suggesting that ICIs modulate the gene expression profile of immune cells more than they modulate the composition of the tumorous and peritumoral immune infiltrate (figures 3 and 4) and this effect encompasses all immune cells (online

supplemental figure 1). Furthermore, we found that different ICIs have both shared and distinct effects on immune cells (figure 4, online supplemental figure 1), and that these effects are dependent on immune preconditioning (figure 5). In fact, treatment with ICIs in the context of concomitant IET resulted in a more extensive regulation of pathways associated with both innate and adaptive immune responses (figure 5).

PTC is the most prevalent human endocrine cancer and treatment with ICIs is being actively explored for the management of patients with advanced, life-threatening disease.<sup>78</sup> Our findings suggest that the presence of IET at the time of treatment with ICIs increases the therapeutic response to ICIs. In our study, we used a basic assessment of therapeutic response: PTC present versus PTC absent. Our study was not sufficiently powered to account for a more detailed classification of tumor burden or aggressiveness. However, the analysis of PTC focality reported in table 1 corroborates the findings from the analysis of PTC presence, and our findings are in line with clinical observations showing that the effect of ICIs on PTC<sup>17-23</sup> and other forms of cancer<sup>8-10 24</sup> is stronger in patients

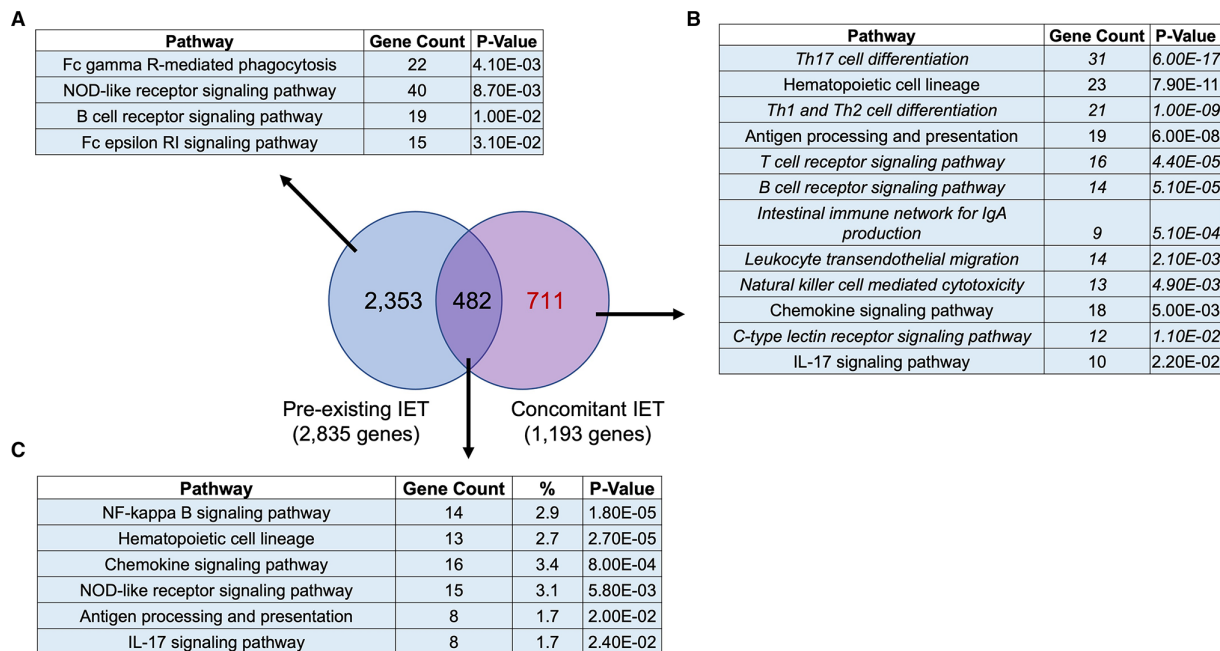


**Figure 5** Concomitant IET is associated with modulation of a specific set of genes enriched in specific innate and adaptive immune pathways. Venn diagram analysis of the 1193 genes modulated by all the tested ICIs in the context of concomitant IET (FDR <0.05) and of the 2835 genes modulated by all tested ICIs in the context of pre-existing IET (FDR <0.05) showed that 2353 genes were modulated only in the context of pre-existing IET, 482 genes were modulated in both conditions and 711 genes were modulated only in the context of concomitant IET. KEGG pathway enrichment analysis of the three sets of genes is reported, respectively in A–C. KEGG pathways in the immune system are reported. A total of 711 genes modulated only in the context of concomitant IET were enriched in several pathways related to innate immunity, adaptive immunity, and immune diseases that were not highlighted in the enrichment analysis of the other two groups of genes. The pathways exclusive to concomitant IET are reported in *italics*. IET, iodine exacerbated thyroiditis.

with thyroiditis. In this respect, it should be noted that, as reported in our prior study with the NOD.H2<sup>h4</sup> TPO-CRE-ER BRAF<sup>G00E</sup> model,<sup>11</sup> animals with pre-existing IET developed PTC with lower frequency than animals without IET or with concomitant IET (figure 2) and they developed mostly unifocal PTC (table 1). This ‘lower tumor burden’ at baseline might have reduced our ability to detect a response to ICI in the presence of pre-existing IET.

To gain insight into the effect of immune preconditioning on the immunomodulatory effect of ICIs, we performed single-cell sequencing of thyroidal CD45<sup>+</sup> cells. Since treatment with ICI can induce thyroiditis,<sup>9,25–29</sup> and thyroiditis significantly increases the number of thyroidal CD45<sup>+</sup> cells, we decided to focus the single-cell sequencing analysis on two of our study arms: concomitant IET and pre-existing IET. We optimized our experimental design to eliminate ‘batch effects’ and maximize our ability to detect both differences between specific ICIs and a ‘class effect’ common to all three ICIs studied. Single-cell sequencing is not an accurate method to assess the prevalence of various cell populations. However, visualization of the immune infiltrates from the various experimental groups provided high-level information about the composition of the thyroidal immune infiltrates in the studied conditions. The fact that in the single-cell analysis pre-existing thyroiditis was associated with an expansion of B cells and T cells (figure 3E and 3A)

is in line with our previous flow cytometry-based analysis in mice with PTC and pre-existing IET versus concomitant IET.<sup>11</sup> The observation that treatment with ICIs does not induce dramatic changes in the composition of the tumorous/peritumoral immune infiltrate is also in line with prior literature.<sup>7,30,31</sup> Confirmation of these prior findings validates our experimental process and gives us confidence in the validity of the additional novel findings of our single-cell analysis, namely the observation that anti-TIM-3, anti-LAG-3, and anti-PD-1 have both specific and shared effects on all the components of the immune infiltrate. This is a novel and important finding (figure 4 and online supplemental figure 1). In fact, to the best of our knowledge, this is the first study that compares the effect of anti-PD-1, anti-TIM-3, and anti-LAG-3 within the same single-cell sequencing library and the first to show that all these treatments modulate gene expression of T cells, neutrophils, macrophages, and B cells (online supplemental figure 1). When zooming in on specific cell types, we lost statistical power. The differences observed across ICI, therefore, appear less impressive in some of the smaller cell populations, such as B cells and T cells in the concomitant IET arm. However, an ICI-specific signature was clearly visible in all the studied cell types, in both experimental arms (online supplemental figure 1).

Our experiment was not powered to detect minor variations in the ability of the three tested ICIs to reduce PTC prevalence, therefore, we cannot comment on the



biological meaning of the genes and pathways uniquely modulated by specific ICIs. However, our histological analysis indicates that all the tested ICIs overall had an ‘antitumor’ effect in the context of concomitant-IET. This justifies our decision to focus on the genes and pathways modulated by all the 3 ICIs in each experimental arm to investigate the tumor-controlling ‘class effect’ of ICIs. Analysis of the genes modulated by all ICIs only in the presence of concomitant IET and only in the presence of pre-existing IET showed many genes uniquely regulated in the presence of pre-existing IET, and a small number of genes uniquely dysregulated in the presence of concomitant IET (figure 5). Remarkably the smaller pool of genes (associated with concomitant IET) was highly enriched in several pathways associated with innate and adaptive immune functions, while the larger pool of genes was not (figure 5). Since the number of single cells analyzed in each library was similar, this is unlikely to be an artifact of statistics and it likely indicates that immune preconditioning (in this case presence of concomitant vs pre-existing IET) strongly modulates the biological effect of ICIs on the immune system.

Our study has additional limitations that should be considered. First of all, we studied a single specific model of PTC, and therefore, the generalization of our findings to other models remains unclear. Second, animals in the pre-existing thyroiditis and concomitant thyroiditis group received ICIs at different ages, with animals in the pre-existing IET group receiving ICIs at an older age than animals in the concomitant IET and no IET groups. This was mandated by our experimental design, but we cannot exclude any potential bias introduced by this age difference. Third, we did not conduct mechanistic studies, which remain to be determined in detail. Finally, we present no human data and therefore the translational relevance of our findings warrants further investigation.

## CONCLUSIONS

ICIs have become a pillar of modern oncology. However, their use remains plagued by significant variability in patient response. The etiological basis of this heterogeneous response remains unknown. Using a murine model that allows temporally controlled induction of PTC and IET we showed that the antitumor effect of ICIs is greater in the presence of concurrent IET. At a molecular level, we showed that the presence of concomitant IET was associated with a stronger ICI-mediated induction of pathways associated with both adaptive and innate immunity. These findings suggest that the biological effect of ICIs is dependent on the immune status or immune preconditioning of the treated individual. These findings support a conceptual framework in which response to ICIs is the result of a balance between the specific drug administered and the immune milieu of the treated patient. Since PTC is the most prevalent endocrine cancer, ICIs are used for the treatment of PTC, and iodine supplementation can induce thyroiditis in humans,<sup>32–35</sup> our findings have

immediate clinical implications. They suggest that induction of iodine-induced thyroiditis might improve response to ICIs in patients with PTC. The fact that the presence of active thyroiditis in the context of treatment with ICIs is also associated with improved prognosis in patients with extrathyroidal tumors<sup>10 36–38</sup> suggests that our findings might be relevant also to other types of cancer. Further studies in other models will be needed to confirm our observations, to understand their mechanistic basis, and to understand the breadth of their clinical relevance.

## Author affiliations

<sup>1</sup>Division of Cardiology, Department of Internal Medicine, The Johns Hopkins University School of Medicine, Baltimore, Maryland, USA

<sup>2</sup>GRC No. 16, GRC Tumeurs Thyroïdiennes, Thyroid and Endocrine Tumors Department; Pitié-Salpêtrière Hospital, Sorbonne Université, Paris, France

<sup>3</sup>Department of Endocrinology and Diabetes, Nagoya University Graduate School of Medicine, Nagoya, Japan

<sup>4</sup>Division of Immunology, Department of Pathology, The Johns Hopkins University School of Medicine, Baltimore, Maryland, USA

<sup>5</sup>Sidney Kimmel Comprehensive Cancer Center, Johns Hopkins University School of Medicine, Baltimore, Maryland, USA

**Twitter** Sylvie T Rousseau @rousseau\_fierce and Luigi Adamo @Luigiadamomdphd

**Acknowledgements** The authors gratefully acknowledge Dr. Hao Zhang, MD, (Johns Hopkins Bloomberg School of Public Health Flow Cytometry and Cell Sorting Core) for assistance with cell sorting, and the Johns Hopkins Sidney Kimmel Comprehensive Cancer Center’s Experimental and Computational Genomics Core, supported by NCI grant P30CA006973, for assistance with the single cell sequencing.

**Contributors** FP and LA designed experiments, performed experiments, and wrote the manuscript. YY designed experiments, performed histology, and wrote the manuscript. SyR and SoR assisted with histology and scoring of thyroid tumors. PC supported the establishment of the study cohort and analyzed all histological sections in blind to define the presence and extent of thyroid cancer. RW and SY helped with the design, execution, and interpretation of the 10X Genomics single-cell gene expression analysis. KB contributed to the statistical analysis. All authors reviewed and approved the manuscript. LA is the author responsible for the overall content of the study.

**Funding** The study was supported by National Institutes of Health grants 5K08HL0145108-03 and 1R01HL160716-01 awarded to Luigi Adamo and by institutional funds of Johns Hopkins University. This work was also supported in part by the National Institutes of Health grant R01 CA-194042 to PC.

**Competing interests** None declared.

**Patient consent for publication** Not applicable.

**Ethics approval** All studies were approved by the Institutional Animal Care and Use Committee (ACUC) of the Johns Hopkins University School of Medicine, under protocol number M020M338.

**Provenance and peer review** Not commissioned; externally peer reviewed.

**Data availability statement** Data are available on reasonable request.

**Supplemental material** This content has been supplied by the author(s). It has not been vetted by BMJ Publishing Group Limited (BMJ) and may not have been peer-reviewed. Any opinions or recommendations discussed are solely those of the author(s) and are not endorsed by BMJ. BMJ disclaims all liability and responsibility arising from any reliance placed on the content. Where the content includes any translated material, BMJ does not warrant the accuracy and reliability of the translations (including but not limited to local regulations, clinical guidelines, terminology, drug names and drug dosages), and is not responsible for any error and/or omissions arising from translation and adaptation or otherwise.

**Open access** This is an open access article distributed in accordance with the Creative Commons Attribution Non Commercial (CC BY-NC 4.0) license, which permits others to distribute, remix, adapt, build upon this work non-commercially, and license their derivative works on different terms, provided the original work is

properly cited, appropriate credit is given, any changes made indicated, and the use is non-commercial. See <http://creativecommons.org/licenses/by-nc/4.0/>.

#### ORCID iDs

Fabiana Pani <http://orcid.org/0000-0003-2566-7971>  
 Yoshinori Yasuda <http://orcid.org/0000-0003-0674-2956>  
 Sylvie T Rousseau <http://orcid.org/0000-0002-8196-5415>  
 Luigi Adamo <http://orcid.org/0000-0003-2704-978X>

#### REFERENCES

- Yang Y. Cancer immunotherapy: harnessing the immune system to battle cancer. *J Clin Invest* 2015;125:3335–7.
- French JD. Immunotherapy for advanced thyroid cancers - rationale, current advances and future strategies. *Nat Rev Endocrinol* 2020;16:629–41.
- Trestini I, Caldart A, Dodi A, et al. Body composition as a modulator of response to immunotherapy in lung cancer: time to deal with it. *ESMO Open* 2021;6:100095.
- Pinato DJ, Howlett S, Ottaviani D, et al. Association of prior antibiotic treatment with survival and response to immune checkpoint inhibitor therapy in patients with cancer. *JAMA Oncol* 2019;5:1774–8.
- Routy B, Le Chatelier E, Derosa L, et al. Gut microbiome influences efficacy of PD-1-based immunotherapy against epithelial tumors. *Science* 2018;359:91–7.
- Chat V, Ferguson R, Simpson D, et al. Autoimmune genetic risk variants as germline biomarkers of response to melanoma immune-checkpoint inhibition. *Cancer Immunol Immunother* 2019;68:897–905.
- Newton JM, Hanoteau A, Liu H-C, et al. Immune microenvironment modulation unmasks therapeutic benefit of radiotherapy and checkpoint inhibition. *J Immunother Cancer* 2019;7:216.
- Baek H-S, Jeong C, Shin K, et al. Association between the type of thyroid dysfunction induced by immune checkpoint inhibitors and prognosis in cancer patients. *BMC Endocr Disord* 2022;22:89.
- Kotwal A, Kottschade L, Ryder M. PD-L1 inhibitor-induced thyroiditis is associated with better overall survival in cancer patients. *Thyroid* 2020;30:177–84.
- Das S, Johnson DB. Immune-related adverse events and anti-tumor efficacy of immune checkpoint inhibitors. *J Immunother Cancer* 2019;7:306.
- Pani F, Yasuda Y, Di Dalmazi G, et al. Pre-existing thyroiditis ameliorates papillary thyroid cancer: insights from a new mouse model. *Endocrinology* 2021;162. doi:10.1210/endo/bqab144. [Epub ahead of print: 01 Oct 2021].
- Bastman JJ, Serracino HS, Zhu Y, et al. Tumor-Infiltrating T cells and the PD-1 checkpoint pathway in advanced differentiated and anaplastic thyroid cancer. *J Clin Endocrinol Metab* 2016;101:2863–73.
- Dierks C, Seufert J, Aumann K, et al. Combination of lenvatinib and pembrolizumab is an effective treatment option for anaplastic and poorly differentiated thyroid carcinoma. *Thyroid* 2021;31:1076–85.
- Solinas C, De Silva P, Bron D, et al. Significance of TIM3 expression in cancer: from biology to the clinic. *Semin Oncol* 2019;46:372–9.
- Beckstead JH. A simple technique for preservation of fixation-sensitive antigens in paraffin-embedded tissues: addendum. *J Histochem Cytochem* 1995;43:345.
- Huang DW, Sherman BT, Lempicki RA. Bioinformatics enrichment tools: paths toward the comprehensive functional analysis of large gene Lists. *Nucleic Acids Res* 2009;37:1–13.
- Chalan P, Di Dalmazi G, Pani F, et al. Thyroid dysfunctions secondary to cancer immunotherapy. *J Endocrinol Invest* 2018;41:625–38.
- Osorio JC, Ni A, Chaff JE, et al. Antibody-mediated thyroid dysfunction during T-cell checkpoint blockade in patients with non-small-cell lung cancer. *Ann Oncol* 2017;28:583–9.
- Okada N, Iwama S, Okuji T, et al. Anti-thyroid antibodies and thyroid echo pattern at baseline as risk factors for thyroid dysfunction induced by anti-programmed cell death-1 antibodies: a prospective study. *Br J Cancer* 2020;122:771–7.
- Basak EA, van der Meer JWM, Hurkmans DP, et al. Overt thyroid dysfunction and anti-thyroid antibodies predict response to anti-PD-1 immunotherapy in cancer patients. *Thyroid* 2020;30:966–73.
- Iwama S, Kobayashi T, Arima H. Clinical characteristics, management, and potential biomarkers of endocrine dysfunction induced by immune checkpoint inhibitors. *Endocrinol Metab* 2021;36:312–21.
- Iwama S, Kobayashi T, Yasuda Y, et al. Immune checkpoint inhibitor-related thyroid dysfunction. *Best Pract Res Clin Endocrinol Metab* 2022;36:101660.
- Kobayashi T, Iwama S, Yasuda Y, et al. Patients with antithyroid antibodies are prone to develop destructive thyroiditis by nivolumab: a prospective study. *J Endocr Soc* 2018;2:241–51.
- Kuiper HM, Brouwer M, Linsley PS, et al. Activated T cells can induce high levels of CTLA-4 expression on B cells. *J Immunol* 1995;155:1776–83.
- Muir CA, Clifton-Bligh RJ, Long GV, et al. Thyroid immune-related adverse events following immune checkpoint inhibitor treatment. *J Clin Endocrinol Metab* 2021;106:e3704–13.
- Cheung Y-MM, Wang W, McGregor B, et al. Associations between immune-related thyroid dysfunction and efficacy of immune checkpoint inhibitors: a systematic review and meta-analysis. *Cancer Immunol Immunother* 2022;71:1795–812.
- Zaborowski M, Sywak M, Nylén C, et al. Unique and distinctive histological features of immunotherapy-related thyroiditis. *Pathology* 2020;52:271–3.
- Muir CA, Wood CCG, Clifton-Bligh RJ, et al. Association of antithyroid antibodies in checkpoint inhibitor-associated thyroid immune-related adverse events. *J Clin Endocrinol Metab* 2022;107:e1843–9.
- Muir CA, Menzies AM, Clifton-Bligh R, et al. Thyroid toxicity following immune checkpoint inhibitor treatment in advanced cancer. *Thyroid* 2020;30:1458–69.
- Ferrari SM, Fallahi P, Galdiero MR, et al. Immune and inflammatory cells in thyroid cancer microenvironment. *Int J Mol Sci* 2019;20. doi:10.3390/ijms20184413. [Epub ahead of print: 07 Sep 2019].
- Mould RC, van Vloten JP, AuYeung AWK, et al. Immune responses in the thyroid cancer microenvironment: making immunotherapy a possible mission. *Endocr Relat Cancer* 2017;24:T311–29.
- Latrofa F, Fiore E, Rago T, et al. Iodine contributes to thyroid autoimmunity in humans by unmasking a cryptic epitope on thyroglobulin. *J Clin Endocrinol Metab* 2013;98:E1768–74.
- Fiore E, Latrofa F, Vitti P. Iodine, thyroid autoimmunity and cancer. *Eur Thyroid J* 2015;4:26–35.
- Rose NR, Bonita R, Burek CL. Iodine: an environmental trigger of thyroiditis. *Autoimmun Rev* 2002;1:97–103.
- Teti C, Panciroli M, Nazzari E, et al. Iodoprohylaxis and thyroid autoimmunity: an update. *Immunol Res* 2021;69:129–38.
- Cohen EEW, Bell RB, Bifulco CB, et al. The Society for immunotherapy of cancer consensus statement on immunotherapy for the treatment of squamous cell carcinoma of the head and neck (HNSCC). *J Immunother Cancer* 2019;7:184.
- Ferris RL. Immunology and immunotherapy of head and neck cancer. *J Clin Oncol* 2015;33:3293–304.
- Fasano M, Corte CMD, Liello RD, et al. Immunotherapy for head and neck cancer: present and future. *Crit Rev Oncol Hematol* 2022;174:103679.